

# Experimental and analytical study on anchorage performance of a new fastening system for wood-frame façade

Alice Le Berder<sup>1</sup>, Van Han Tran<sup>1</sup>, Tuan-Anh Nguyen<sup>1</sup>, Clémence Lepourry-Nicollet<sup>2</sup>, Hugues Somja<sup>1</sup>

<sup>1</sup> INSA de Rennes LGCNM/Structural Engineering Research Group, France, alice.le-berder@insa-rennes.fr, Van-Han.Tran@insa-rennes.fr, tuan-anh.nguyen2@insa-rennes.fr, hugues.somja@insa-rennes.fr

<sup>2</sup> INGENOVA, Civil Engineering Office, France, clemence.nicollet@groupe-legendre.com

## Abstract

Wooden frame façades (WFFs) are increasingly popular in concrete construction, due to their lower carbon footprint compared to traditional concrete façades. However, designing robust fastening systems for WFFs remains a challenge. This study investigates the anchorage performance of an innovative fastening system for WFFs that utilizes a steel U-profile assembly partially embedded in concrete. An experimental campaign is conducted on four specimens with different U-profile configurations under simulated wind loads. The results indicate that failure is governed by the concrete slabs, with cracks propagating outward the U-profile to create cone-shaped fractures. The key factors influencing anchorage resistance are identified as embedment depth and concrete compressive strength. A predictive formula is developed to estimate anchorage resistance.

## 1 Introduction

In France, since the entry into force of the environmental regulation RE2020 [1], buildings increasingly combine a primary concrete structure with wood-framed façades to reduce their carbon footprint. In usual practice, these prefabricated façades are installed after the construction of the primary structure, using metal brackets fixed to the concrete edge with anchor bolts. However, this practice slows the construction process and does not allow for precise altimetric adjustments. Irregularities are corrected with wedges, a method that induces many quality defects.

INGENOVA, the R&D entity of the French construction company GROUPE LEGENDRE, in collaboration with the engineering school INSA Rennes, has conceptualized an integrated construction process, associated to a specific fastening system (see Figure 1). The construction process is conceived in such a way that all operations are made by concrete workers. The lower façade serves as framework for the slab. The fastening system is fixed to the lower façade and is embedded in the slab when concreting it. Then, the level of upper brackets is adjusted, and the upper timber façade is installed.

The fastening, shown in Figure 2, is a metal assembly composed of four parts joined together by bolts: an anti-tilt bracket serving as support of the lower façade, a U-shaped part that will be embedded in the concrete in order to ensure the anchorage of the system, and a load-bearing bracket for the upper façade, fixed to the U-shaped profile through an adjustment plate allowing to mitigate the level of the bracket.

One of the issues of the fastening system is to ensure an anchorage in the concrete strong enough to transfer the wind loads and the dead loads of the façades to the slab. The anchorage is here provided by cuts in the flanges of the U part. The cutouts filled with concrete enable the formation of a shear connector, commonly known as a perfobond shear connector [2]. This type of connector is designed to transfer shear forces between steel and concrete by combining mechanical interlock, friction, and reinforcement, ensuring effective composite action. While it is widely used in steel-concrete composite beams, such as in bridges and high-rise buildings, it has not yet been applied as a fastening system for façades. Moreover, the geometry of the fastening differs from usual perfobond configurations. Consequently, the anchorage of the U part requires an experimental characterization.

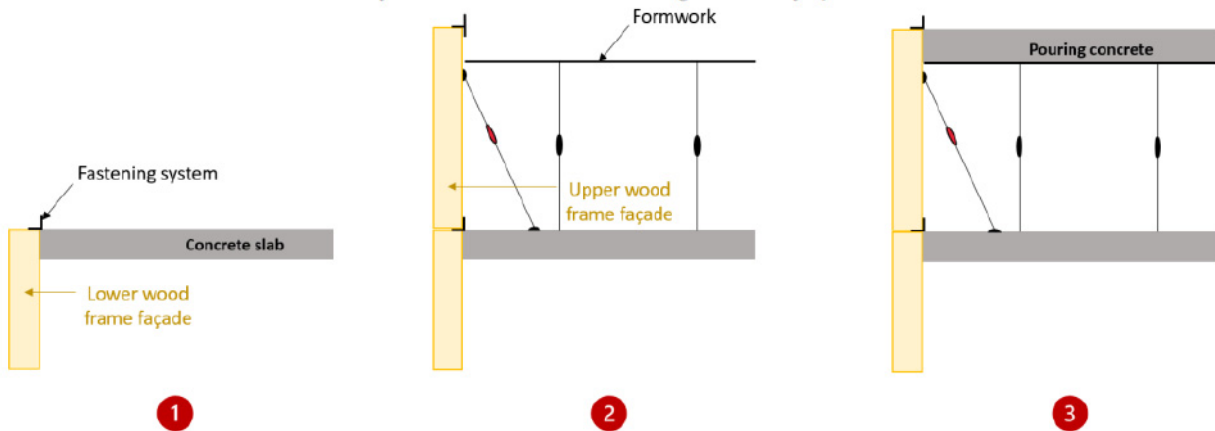
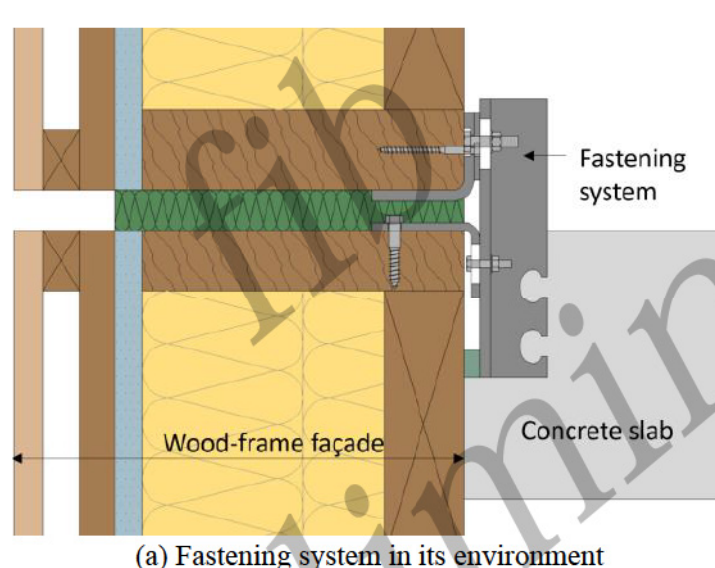
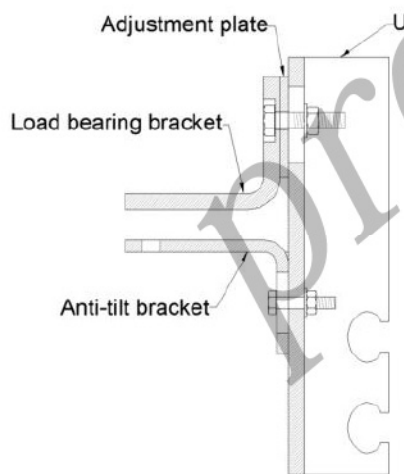


Figure 1: Construction process

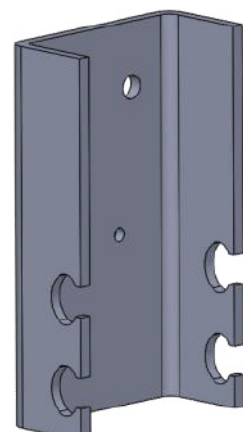
The objective of the study presented in the paper is thus to investigate experimentally the steel-concrete anchorage resistance, and to try to deduce a design formula setting in evidence the effect of the main geometrical and mechanical parameters on the resistance. First the different experimental campaigns exploring different versions of the U-shape profile will be presented, before developing a simple analytical design formula.



(a) Fastening system in its environment



(b) Components



(c) Detail of the U part

Figure 2: Steel parts of the fastening

## 2 Experimental testing

The tests examined the anchorage performance of the proposed fastening system for wooden frame façades (WFFs) embedded in structural slabs under façade-induced loads. To achieve this, various configurations of the system were developed and evaluated under the most critical loading condition: the wind in depression or suction wind load.

### 2.1 Test specimens

Four test specimens featuring fixing U-profiles—designated as P, PM, MC, and MC HA—were evaluated in this study, as depicted in Figure 3. Each specimen consisted of two concrete blocks with U-profiles embedded to a depth of 110 mm into the concrete, see Figure 4 and Figure 5. The U-profiles were fabricated from steel plates measuring 112 mm in width and 189.5 mm in height. These plates were extended with two flanges bent at a 90° angle, each flange measuring 50 mm in depth, and included two cutouts on the flanges. The key differences between the U-profiles were the dimensions of the cutouts and the embedment depth ( $h_1$  and  $h_2$ ) of these cutouts into the concrete blocks.

The P U-profile featured two circular cutouts with a diameter of 20 mm and a maximum embedment depth ( $h_1$ ) of 40 mm. The PM U-profile was created by expanding the upper circular cutout of the P U-profile horizontally by an additional 10 mm ( $W_e$ ). The MC U-profile had notched cutouts with a maximum embedment depth ( $h_1$ ) of 46 mm. In the MC HA specimen, an additional rebar was incorporated horizontally through the cutout holes, as enhanced reinforcement.

To simulate structural slabs, the concrete blocks were designed with dimensions of 600 mm in height, 460 mm in width, and 200 mm in thickness. Reinforcement bars were embedded within the concrete blocks.

The fixing U-profiles for the specimens were fabricated at the Ouest Préfa workshops, while the concrete pouring and specimen preparation were conducted at the INSA Rennes laboratories. The reinforcement incorporated steel bars of types HA6, HA8, and HA10. Figure 4 provides detailed specifications of the specimens, including the dimensions and reinforcement of the two concrete blocks.

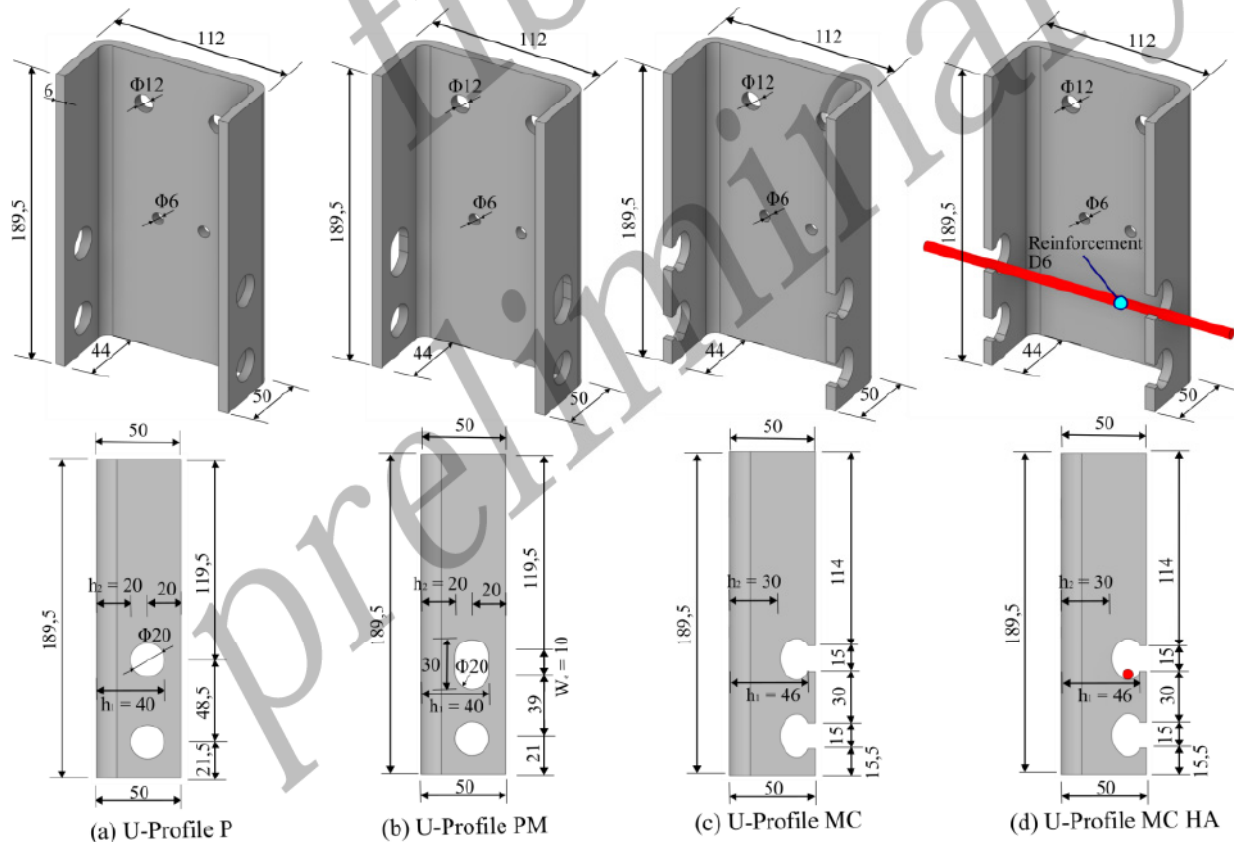


Figure 3: FACILA fixing U Profile specimen

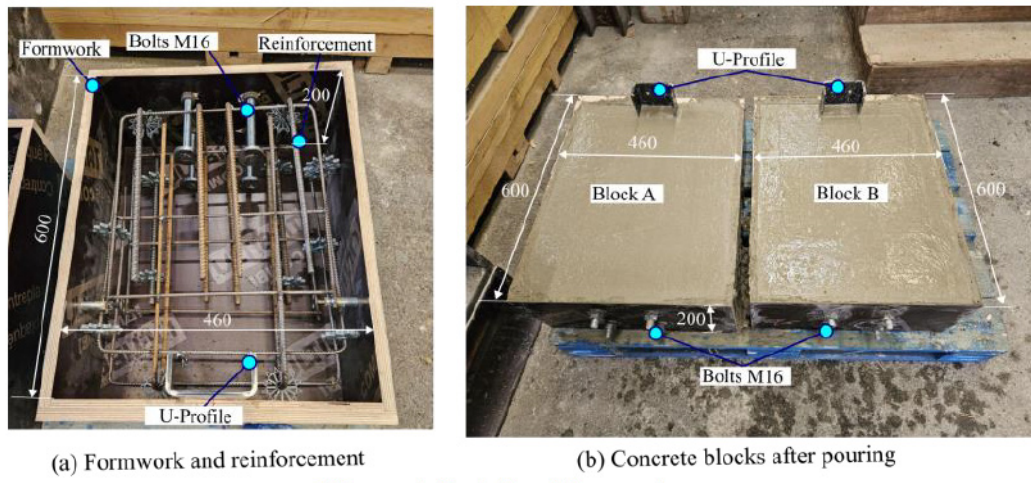


Figure 4: Details of the specimens

## 2.2 Test setup

The test setup (see Figure 5) simulated wind loading conditions by positioning the U-profile and concrete block assembly horizontally, aligning with the vertical loading direction. Vertical loads, representing wind pressures, were applied using a hydraulic jack and transmitted through an interface piece at the center of the HEB 100 loading beam. These loads were distributed via two hinged connections fastened to a T-connector with two bolts.

The T-connector, secured to the U-profile using M10 bolts, directed the applied load to the U-profile surface. Each test specimen, consisting of two concrete blocks and U-profiles, was supported by two HEB 220 columns and positioning beams. The concrete blocks were anchored to the steel columns using eight M16 bolts, providing stability and ensuring precise load application during the testing process.

Four tests were conducted under suction wind load conditions ( $W^-$ , load applied upwards), applying a consistent loading protocol with varying load values to align with the Serviceability Limit State (SLS) level for each specimen. Initially, two cycles were performed between 0 and 5 kN, followed by 25 SLS cycles before proceeding to failure loading. The hydraulic jack was operated in displacement-control mode at a rate of 2 mm/min.

## 2.3 Instrumentation

Four displacement sensors (LVDTs), labeled C1, C2, C3, and C4, were utilized to measure the vertical deformation of the specimens during testing. These sensors were consistently positioned across all tests, mounted on the free section of the U-profile, and maintained at a fixed horizontal distance of 50 mm from the concrete face, as shown in Figure 5.

## 2.4 Material properties

The compressive strength of the concrete blocks for each specimen was evaluated by testing three concrete cylinders (110 mm x 220 mm) following the guidelines outlined in EN 12390-3 [3], at the day of the test. The average compressive strength,  $f_{cm}$ , obtained from these tests, are summarized in Table 1.

Additionally, the mechanical properties of the steel components used in the specimens were assessed through tensile testing conducted in accordance with ISO 6892-1[4]. This included fixing U-profiles, which were fabricated using S235 steel.

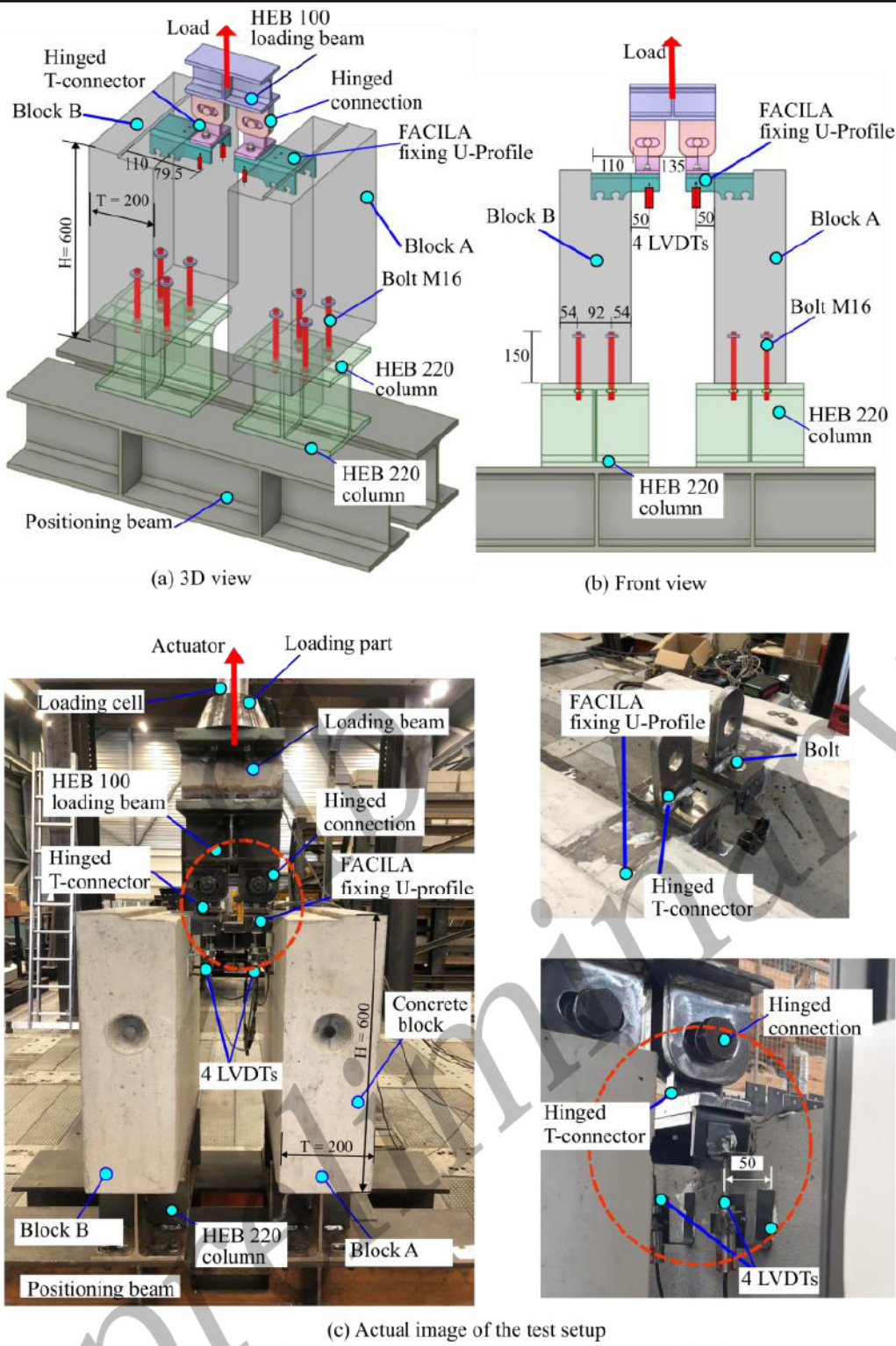


Figure 5: Test setup and measurement instrumentation.

Table 1: Concrete properties

	Elastic modulus (MPa)	Average strength $f_{cm}$ (MPa)
Concrete P specimen	34800	27.1
Concrete PM specimen	34800	28.4
Concrete MC specimen	34800	24.7
Concrete MC HA specimen	34800	27.8

### 3 Experimental results

#### 3.1 Failure mode and crack patterns

The experimental investigation revealed consistent failure mechanisms across all four tests with the different U-Profile configurations. These failures were primarily governed by the behavior of the concrete blocks rather than the fixing U-Profiles, which exhibited no signs of yielding during testing. The failure mode was characterized by the initiation of cracks near the flanges of the U-Profiles and the edges of the concrete blocks. As the applied load approached its peak, these cracks propagated outward, forming a cone-shaped fracture surrounding the embedded U-Profiles. The cracks extended from the flanges of the U-Profiles toward the outer edges of the concrete blocks, as illustrated in Figure 6a–d.

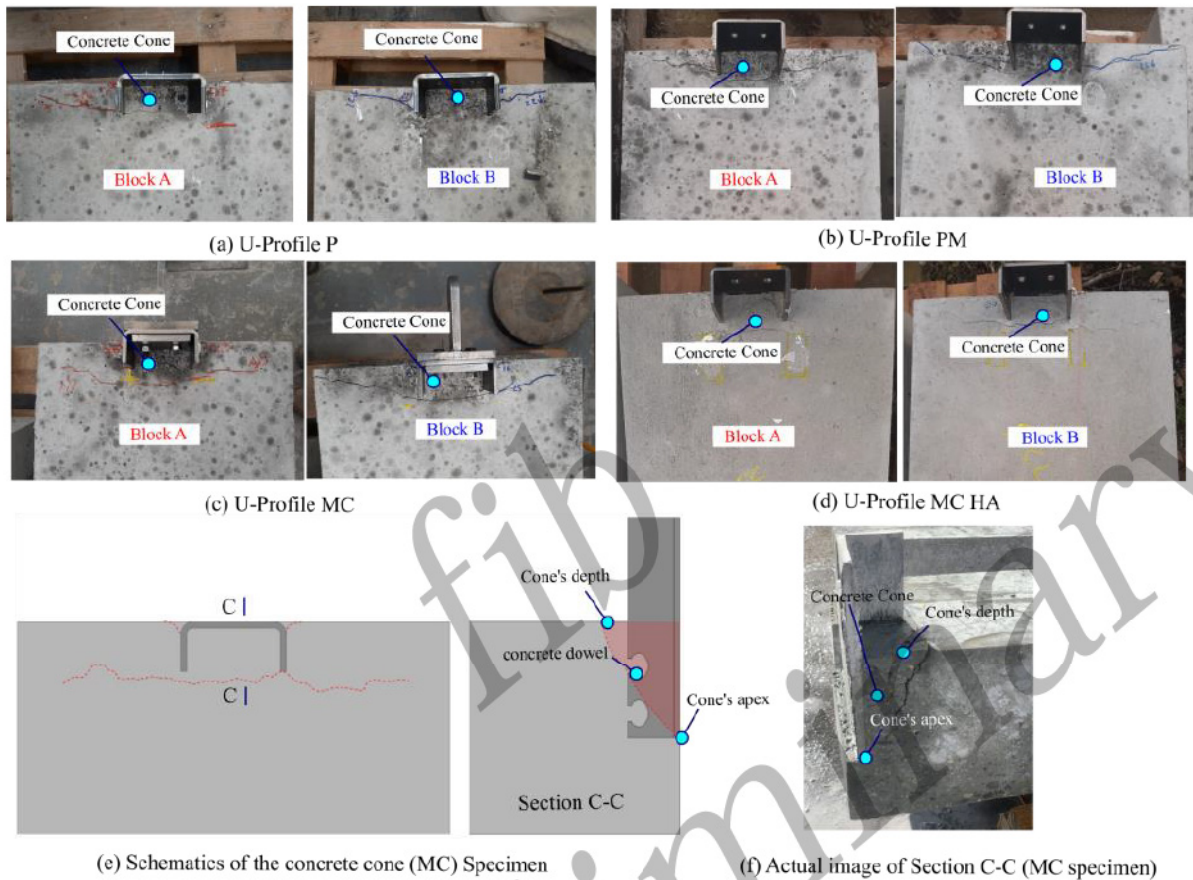


Figure 6: Failure mode and crack patterns of four specimens

Observations from the cross-section C-C of the MC specimen (Figure 6e–f) revealed essential details about the formation of the concrete cone. The cone's apex was located at the outer edge of the concrete base, where it intersected with the bottom of the U-Profile. The cone's depth extended through the concrete dowels formed within the cutouts of the U-Profiles, and the cone's depth at the surface of the concrete block was approximately equal to the flange width of the U-Profiles.

The results highlight that the depth of the concrete dowels formed within the cutouts of the U-Profiles is the most significant factor affecting anchorage resistance. Specimens PM and P displayed similar concrete cone patterns, indicating that increasing the width of the cutout holes ( $W_e$ ) in the U-Profiles did not substantially influence the failure mode of the specimens. This finding suggests that variations in cutout width have minimal impact on the effective volume of the load-bearing concrete cone.

Conversely, specimens MC and MC HA exhibited larger concrete cones compared to PM and P, as evidenced by the broader cracks observed on the surfaces of the concrete blocks. This observation confirms that increasing the embedment depth ( $h_1$  and  $h_2$ ) of the concrete dowels within the U-Profiles significantly enlarges the concrete cone, which is directly correlated with enhanced load-bearing capacity. Despite the inclusion of perforated rebar in the MC HA specimen, its failure mode remained

comparable to that of MC, showing that the addition of rebar within the cutouts has a negligible impact on structural performance.

These findings underscore the critical role of embedment depth in enhancing anchorage resistance, while variations in cutout width and the inclusion of rebar within the cutouts exhibit limited influence on the overall structural performance.

### 3.2 Load-deflection response

Figure 7 presents the test results for the four specimens subjected to wind loading, each featuring a unique U-profile configuration. The results are depicted as a force-displacement graph, with displacement values calculated as the average of measurements obtained from the four LVDTs.

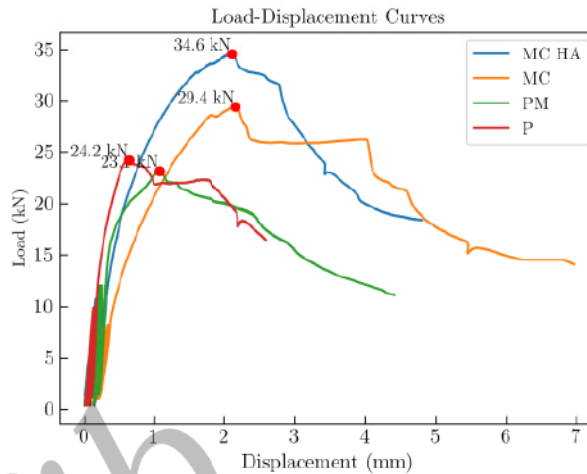


Figure 7: Load – displacement curves of the specimens

The configuration of the cutouts in the fixing U-profiles and the compressive strength ( $f_c$ ) of the concrete blocks significantly influence the structural performance of the specimens.

For the P and PM specimens, which share identical embedment depths ( $h_1$  and  $h_2$ , as shown in Figure 3), the maximum loads were similar, at 24.2 kN and 23.1 kN, respectively. This consistency aligns with the comparable compressive strengths of the concrete blocks ( $f_c = 27.1$  MPa for P and  $f_c = 28.4$  MPa for PM). The slight reduction in load capacity observed in the PM specimen may perhaps be attributed to the increased cutout width ( $W_e = 10$  mm). This widened cutout did not enhance the volume of the load-bearing concrete cone; instead, it led to a small increase in displacement at the peak load and a reduction in stiffness in the load-displacement curve.

For the MC HA specimen (maximum load = 34.6 kN) and the MC specimen (maximum load = 29.4 kN), the addition of a reinforcing bar within the cutout did not significantly improve structural performance. Both specimens exhibited similar displacements at their peak loads, approximately 2 mm. The higher load capacity of the MC HA specimen is primarily attributed to its higher concrete compressive strength ( $f_c = 27.8$  MPa) compared to the MC specimen ( $f_c = 24.7$  MPa). This suggests that the load resistance is predominantly derived from the concrete cone surrounding the U-profiles, with the inclusion of reinforcement within the cutouts having minimal impact on structural performance.

A comparison between the P and MC HA specimens, which exhibit nearly identical concrete compressive strengths ( $f_c = 27.1$  MPa and  $f_c = 27.8$  MPa, respectively), highlights the influence of embedment depth. The greater embedment depth of the MCL HA specimen ( $h_2 = 46$  mm) compared to the P specimen ( $h_2 = 40$  mm) resulted in a 43% increase in peak load, from 24.2 kN to 34.6 kN. This enhancement is attributed to the larger effective volume of the load-bearing concrete cone, which plays a crucial role when the U-profiles are subjected to wind loads.

These findings emphasize that the embedment depth of the cutouts and the compressive strength of the concrete are critical factors influencing structural performance, while the addition of reinforcement within the cutouts has a negligible effect. The results provide a foundation for the development of an analytical model to estimate the anchorage resistance of U-profiles embedded in concrete slabs under wind loads. This analytical model, which accounts for the effects of embedment depth and concrete compressive strength, is presented in Section 4.

## 4 Prediction of the anchorage resistance

### 4.1 Design models for similar systems

Existing studies on PERFOBOND-type connectors primarily focus on predicting the longitudinal shear capacity, with several analytical and empirical equations developed for this purpose [5], [6], [7]. In contrast, pull-out capacity, which is more directly related to the functioning of the fastener, has been addressed in only limited number of studies. Zheng et al. [8], for example, proposed equation (1) based on pull-out tests and a parametric study to calculate the tensile resistance of a notched perfobond connector with a rebar in the hole:

$$N_r = \gamma_w [0,95(d_h^2 - d_r^2)f_c + 0,45d_r^2f_{ry} + 0,18d_h t_p f_{sy}] \quad (1)$$

where  $\gamma_w$  is the influence factor of the notch,  $d_h$  is the hole diameter (mm),  $d_r$  is the rebar diameter (mm),  $f_c$  the concrete compressive strength (MPa),  $f_{ry}$  is the rebar yield strength (MPa),  $t_p$  is the thickness of the metal plate and  $f_{sy}$  is the metal plate yield strength (MPa), (see Figure 8).

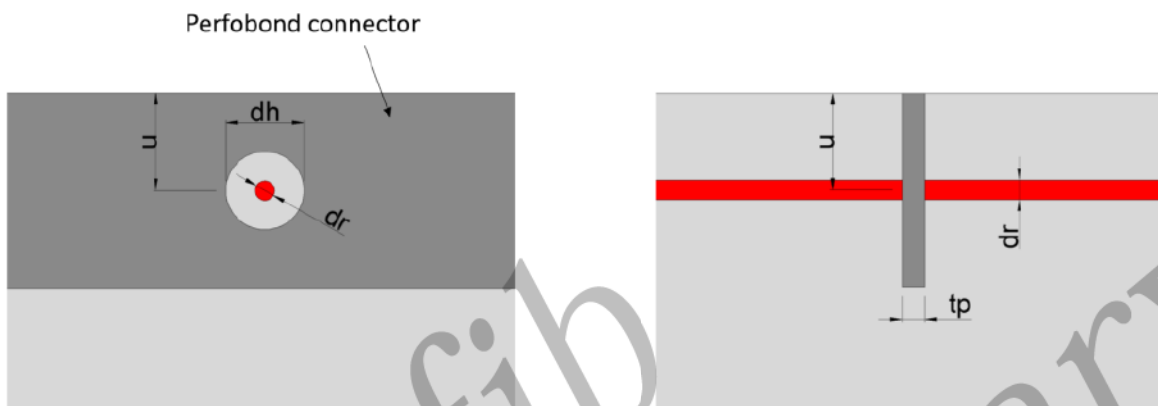


Figure 8: Perfobond connector embedded in concrete

The first term of the equation refers to the contribution of the concrete dowel, the second term accounts for the contribution of the reinforcing bar in shear, and the third term corresponds to the contribution of the metal plate.

More recently, Lipeng et al. [9] have investigated the pull-out performance of PERFOBOND connectors used in high-strength concrete. An experimental campaign and a numerical parametric study were used to establish an analytical model of the pull-out resistance, as expressed in Equation (2):

$$N_r = (3u + d_h)^2 \cdot 3 \left( u + \frac{d_h}{3} \right)^{-0,56} \sqrt{f_c} \quad (2)$$

According to this equation, the tensile resistance of the perfobond connector depends on the following three parameters:  $u$ , the embedded depth (mm),  $d_h$ , the hole diameter, and the concrete shear resistance, given by the square root of the compressive resistance of concrete.

The fastening system can also be compared with headed stud connectors, that have been widely studied in the literature. Their resistance under a tensile load can be computed through the current standard EN 1992-4 [10]. In this standard, the tensile resistance is calculated according to the failure mode. The tensile resistance equation in case of concrete cone failure is given by Equation (3):

$$N_r = k_1 \sqrt{f_c} h_{ef}^{1,5} \frac{A_{c,N}}{A_{c,N}^0} \Psi_{s,N} \Psi_{re,N} \Psi_{ec,N} \Psi_{M,N} \quad (3)$$

Where  $k_1$  is a coefficient that depends on the state of cracking of concrete,  $h_{ef}$  (mm) is the effective embedment depth,  $A_{c,N}$  ( $\text{mm}^2$ ) is the reference projected area,  $A_{c,N}^0$  ( $\text{mm}^2$ ) is the actual projected area limited by overlapping concrete cones, and the  $\Psi$  factors account for various effects, including edge distances, reinforcement, group effects, and compression forces due to bending moments.

While the above equations provide valuable insights into the tensile resistance of existing connectors, there is still a need for a comprehensive analytical approach tailored to the unique characteristics and behavior of the proposed fastening system. A predictive formula has been developed and will be presented in the following section.

## 4.2 Proposed equation

Experimental tests (presented in earlier sections) on configurations P, PM, MC, and MC HA revealed that concrete compressive strength and embedment depth are the primary factors influencing anchorage resistance. Specifically, we observed that incorporating a rebar crossing the U-profile cutout, increasing the cutout area, and plastic deformation of the Perfobond steel had negligible effects on resistance. Based on these findings, the proposed design formula accounts only for the embedment depth and the compressive strength of the concrete, omitting other factors due to their minimal or negligible contributions to anchorage resistance.

It is inspired from the anchorage resistance equation given by the EN 1992-4 [10] in case of a concrete cone failure: it depends on the square root of the compressive strength  $\sqrt{f_c}$  and on an equivalent anchoring depth noted  $h_{eq}$  (mm), raised to the power of 1.5. These dependencies can be considered as consistent with the formula of Lipeng et al. [9] (Equation (3)), with less sophistication.

The equation is deduced from the moment equilibrium of the U part: it is assumed that the moment created by the application of the force F is balanced by the shearing of concrete in the upper dowels noted  $R_a$  and the compression of the concrete against the web of the U in its lower part noted  $R_b$  as shown in Figure 9 (a). The resulting compression force  $R_b$  is positioned 5 mm from the end of the U. Thus, the anchorage resistance force is expressed by the following equations:

$$F_r = \frac{\alpha h_{eq}^{1.5} \sqrt{f_c} l_1}{l_2} \quad (4)$$

With:

$$h_{eq} = \beta h_{min} + (1 - \beta) h_{max} - \Delta \quad (5)$$

$l_1$  is the distance between the force F and the reaction  $R_b$  (mm),  $l_2$  is the distance between the middle of the upper dowel and the reaction  $R_b$  (mm),  $\alpha$  is a calibration coefficient,  $\beta$  is a coefficient that mitigates the equivalent anchoring depth from the distances  $h_{min}$  and  $h_{max}$  (see Figure 9 (b)),  $h_{eq}$  is the equivalent height, and  $\Delta$  is a distance that also calibrates the anchoring depth (mm).

The parameters  $\alpha$ ,  $\beta$ , and  $\Delta$  were determined through linear regression analysis based on the experimental results, yielding the following values:  $\alpha = 32.7$ ,  $\beta = 0.6$ , and  $\Delta = 8$  mm.

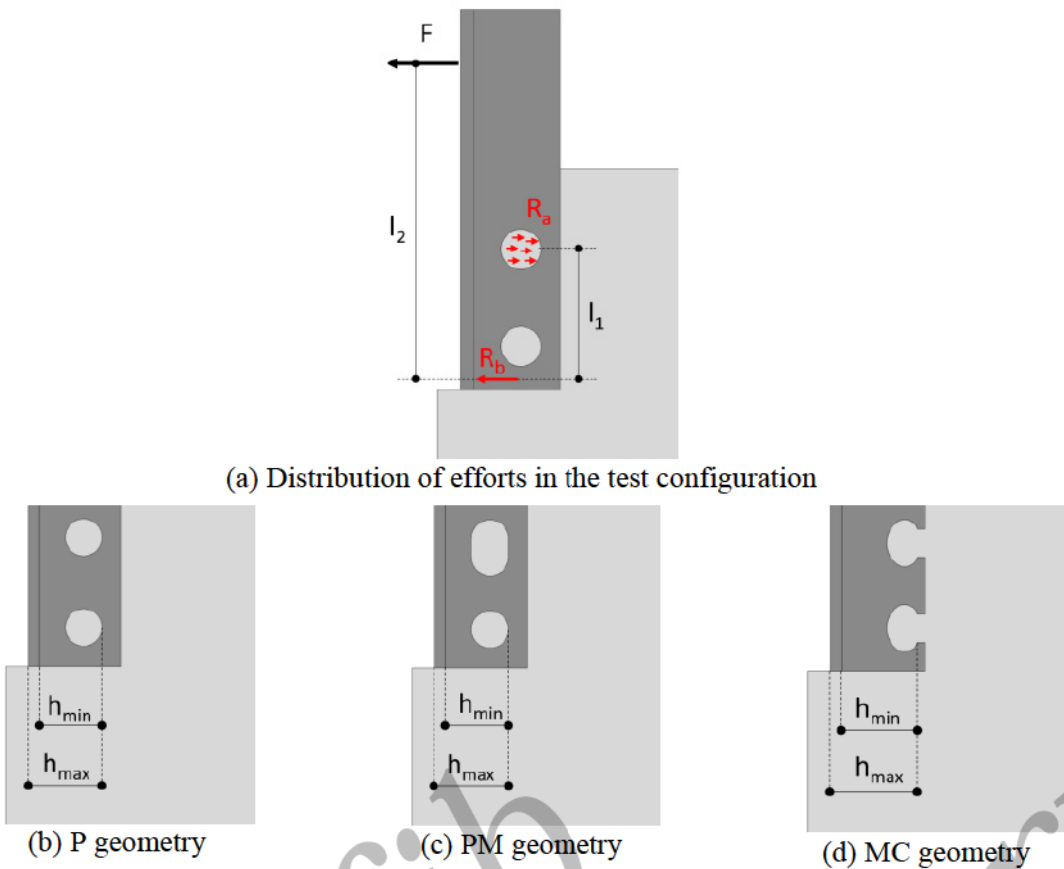


Figure 9: Assumptions and parameters considered in the calculation of anchoring resistance.

#### 4.3 Validation

As presented in Figure 10, the calculated anchoring resistance from Equation (4) is compared to the experimental results. The analytical model shows a strong correlation with the anchorage resistance obtained from the experimental study. The relative deviations between the experimental and predicted values are minimal, ranging from 0.1% to 1.2%, highlighting the model's accuracy and reliability under the tested conditions.

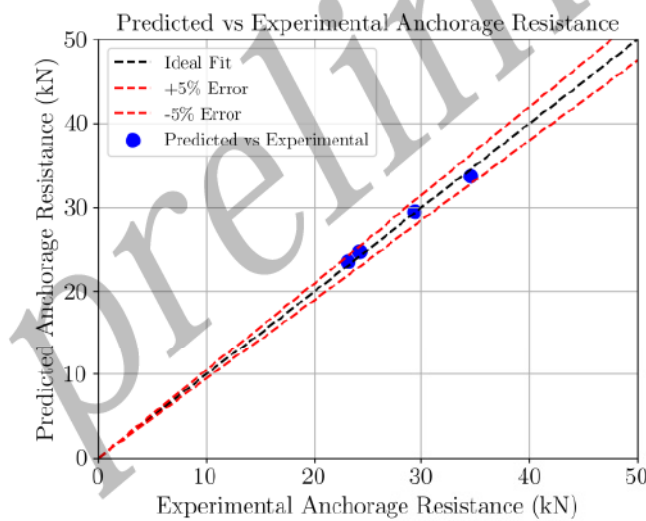


Figure 10: Verification of the analytical model by comparison with experimental results

Therefore, Equation (4) can be used to estimate the anchorage resistance of the fastening system when the geometrical characteristics of the connectors are close to those of the tests.

It should be noted that this design formula is only valid for cone-type failures; other failure modes, such as splitting or crushing, may require alternative approaches. Moreover, the number of experimental tests is limited. Thus, the proposed formula should be considered as a guidance tool for optimizing the shape of the embedded zone. If the dimensions of the system need to be altered, a new experimental campaign will be mandatory.

## 5 Conclusion

This study experimentally examined the anchorage behavior of an innovative fastening system for wood-frame façades (WFFs) integrated in concrete structures. It is based on a steel U-shaped profile placed at the edge of the slabs, with flanges embedded in the concrete. The anchorage in the concrete is ensured by perfobond-type cutouts in the flanges. Four test specimens featuring different U-profile configurations were analyzed, with a focus on critical parameters such as embedment depth, cutout dimensions, and concrete compressive strength. While the conclusions are specific to the scope of this study, key insights include:

- The failure of the specimens was primarily governed by the concrete blocks, with cracks initiating around the embedded U-profiles and propagating outward to form a cone-shaped fracture.
- Embedment depth and concrete compressive strength were identified as the primary factors influencing anchorage resistance. Deeper embedment depths increased the effective volume of the concrete cone, resulting in higher load-bearing capacities.
- Increasing the cutout width had negligible influence on the anchorage resistance, as it did not contribute to the effective volume of the concrete cone.
- The addition of a rebar within the cutout did not significantly enhance structural performance, as the load-bearing capacity was primarily derived from the concrete cone surrounding the U-profile.
- A formula derived from Eurocode EN 1992-4 [10], incorporating embedment depth and concrete compressive strength, was utilized to estimate the anchorage resistance. The model demonstrated strong alignment with the experimental results, offering a reliable framework for optimizing the design of the connector.

This study highlights the critical role of embedment depth and concrete strength in the structural performance of U-profile anchorage systems, while emphasizing the limited impact of cutout modifications and reinforcement bars. These findings form a foundation for designing efficient and reliable fastening systems for wood-frame façades in sustainable construction. Future research could explore additional U-profile configurations to further enhance the structural performance of the fastening system and develop corresponding formulas to refine anchorage resistance predictions.

## Acknowledgements

The authors gratefully acknowledge financial support from the French National Research Agency (ANR, Paris) with grant number ANR-21-CHIN-0003 through the ANR FREEINBTP project.

## References

- [1] Ministère aménagement du territoire transition écologique, «Réglementation environnementale RE2020,» 2022.
- [2] F. Leonhardt, W. Andrä, H.-P. Andrä et W. Harre, «New improved shear connector with high fatigue strength for composite structures (in german),» *Beton und stahlbetonbau*, 1987.
- [3] EN 12390-3. Testing hardened concrete—Part 3: Compressive strength of test specimens. 2009.

- [4] ISO 6892-1. EN ISO 6892-1: 2017-02: Metallic materials-Tensile testing-Part 1: Method of test at room temperature. 2017
- [5] S. Zheng, Y. Liu, Y. Liu et C. Zhao, «Experimental and numerical study on shear resistance of notched perfobond shear connector,» *MDPI*, 2019.
- [6] E. C. Oguejiofor et M. U. Hosain, «Numerical analysis of push-out specimens with perfobond rib connectors,» *Computer & Structures*, pp. 617-624, Mai 1995.
- [7] M. R. Veldanda et M. U. Hosain, «Behaviour of perfobond rib shear connectors : push-out tests,» *Canadian Journal of Civil Engineering*, février 1992.
- [8] S. Zheng, Y. Liu, Y. Liu et C. Zhao, «Experimental and parametric study on the Pull-Out Resistance of a Notched Perfobond Shear Connector,» *Applied Science*, February 2019.
- [9] L. Sun, Y. Liu, F. Shi et H. Wang, «Pull-out performance of perfobond rib connectors in steel high-strength concrete composite bridge pylons,» *Construction and Building Materials*, December 2022.
- [10] CEN European Committee for Standardization, «Eurocode 2 - Design of concrete structures - Part 4: Design of fastenings for use in concrete,» 2018.